Method for building's thermal flexibility in a multi energy vector district

Mathieu Brugeron[b], Mathieu Vallée[b], Antoine Leconte[a], Aurélie Foucquier[a], Adrien Brun[a]

[a] *Université Grenoble Alpes, CEA, Liten, INES, DTS, 73375 Le Bourget du Lac, France, firstname.lastname@cea.fr*

[b] *Université Grenoble Alpes, CEA, Liten, INES, DTCH, 73375 Le Bourget du Lac, France, firstname.lastname@cea.fr*

Abstract:

This article describes thermal flexibility of building methods at a district level considering different level of details of building models, illustrated by a case study in a newly built district in Grenoble. Heat represents a huge part of final consumption (81% for the residential sector, 60% for the industry), so district heat networks represents a major action lever towards energy transition. In previous work, a mix thermal and electric architecture has been designed and described at district level. This architecture has been upgraded to simulate the thermal building flexibility and integrate model-predictive controllers. Therefore, this upgrade considers a tool for co-simulation between an optimization problem modeler and several simulation models (an electric model and a set of models for the thermal simulation). On the optimization side, we considered one to eight buildings to be flexible in the district, and assess the impact of its flexibility on the system. A refinement of their flexibility potential is one difficult key aspect of this study, considering a complex multi-vector MILP model. The calibration process has been developed in order to identify the optimization model of this flexible equivalent building. On the simulation side, the simulation models are divided into: the production, the heat network, the heat distribution at building level and the building.

Keywords:

Thermal Flexibility, Multi-vector energy, district scale, Co-simulation, MPC.

1. Introduction

In a context of climate change, research in the efficient energy management field have greatly improved.

Complexity in the energy network have raised by including more and more renewable energies at a local scale [1], a deeper coupling between different energy vectors [2] and a multiplicity of storage system [3]. Aiming a reduction of the carbon emission, building, especially residential building, represent a massive impact as a third of the global energy consumption and a quarter of the carbon emissions [4]. To tackle this factual state according to the energy context, researchers are currently studying a new approach considering the building as a flexible element in energy systems.

2. State of the art

Considering its thermal inertia, building can be a flexibility tool in the same way as Electrical Vehicles in the control strategy at district scale. Its impact grew by considering coupling network such as thermal-electrical coupling. In order to integrate flexibility of buildings, solutions such as cosimulation ([5], [7], [8]) or aggregation ([6], [8], [11], [12]) have been explored. The main issue is the complexity of the model that can be:

- Physical model, with different levels of complexity ([5], [6], [7], [10], [11], [12])
- Data-based model driven from physical simulation ([8], [9])

Considering the aggregated approach, despite solid results and processes, it seems lacking some level of fineness in the study of flexibility of each building at district scale. On the cosimulation side, a classic control is applied which have proven its robustness but is not perfectly adapted to flexibility.

Thus, in this article, we propose to study the impact of thermal flexibility of building at district scale, with an individual approach for building simulation. We enhance a cosimulation process including Model Predictive Control (MPC) [13] in the loop in order to take benefit from the flexibility approach.

First, we present the main tool and method included in the cosimulation approach carried by the cosimulation engine PEGASE. Then, we present the theoretical aspects of the multi-vector cosimulation via the thermal models, the electrical models and the Mixed Integer Linear Programing (MILP) model used to determine the

https://doi.org/10.52202/069564-0251

optimised control strategy. Finally, we present a use case based on a real district Cambridge in which we study the impact of thermal flexibility from none to ten building.

3. Tools and methods

In this section, we present the methods and tools used in our work.

This work focuses on the management of district energy systems providing electricity and heat (Domestic Hot Water DHW and Space Heating SH) through a coupling between electric and heat network including renewable energy and storage.

3.1. Multi-Energy Networks Case Study

To illustrate our approach, we use a district-scale multi-energy network case study presented in previous works ([13], [14], [15]). This case study is inspired from the Cambridge district, based in Grenoble: it takes into account the electric, space heating (SH) and domestic hot water (DHW) needs of the buildings, and the objective is to satisfy them is an optimal way using a combination of renewable energy sources, storage and district heat network and the power distribution grid. Table 1 recalls some of the energy systems considered. A more detailed description of the case study can be found especially in [15].

Table 1. List of the energy system considered in this work.

Production	Storage	Loads
Photovoltaic panels	Battery	Electric loads from building
Cogeneration	Thermal Energy Storage	Heat loads
Heat pumps	Fuel cells	DHW consumption
Solar panels	Electric Vehicles	
Gas Boiler		

In the current work, we especially study the impact of thermal flexibility at building level on the energy management at district level.

3.2. Co-simulation and Model-Predictive Control Approach

In order to account for the dynamic behaviour and complex control of such a multi-energy coupled system, we use a co-simulation and model-predictive control (MPC) approach. More precisely, we use the PEGASE tool [15] to couple an optimisation model with several dynamic simulation models it controls. Thanks to the cosimulation process, a complex multi-vector system at district scale can be scattered into several subsystems, for which specific software are chosen.

Figure 2 shows the overall process and presents the main components involved:

- A model of the electric distribution network (“Electric Model”), including photovoltaic (PV) production and electricity storage
- Three thermal models, for the District Heating production systems (“DHN Model”, standing for District Heating Network model), for the buildings (“Building Model”) and for the internal heat distribution in the building (“HDC Model”, standing for Heat Distribution Circuit).
- An optimisation model, based on the Mixed Integer Linear Programming (MILP) formalism (“MILP Problem Solver”)

All dynamic simulation models are encapsulated using the standard Functional Mock-up Interface. To perform the MPC process, the MILP problem is solved recursively with a rolling horizon, using a commercially available MILP solver (see [15] for details).

https://doi.org/10.52202/069564-0251

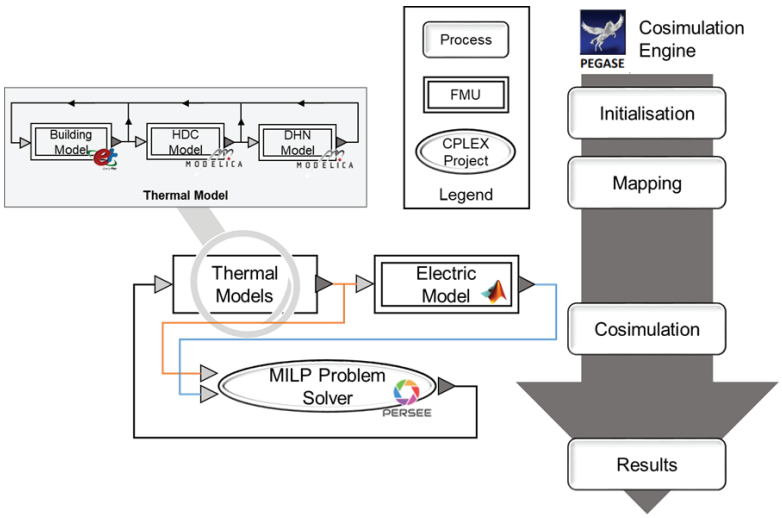

Figure 1. General principles of co-simulation driven multi-vector energy management. (Source: Authors)

3.3. Dynamic simulation models

This section describes more in details the dynamic simulation models used in the case study. It should be noted that these models are designed in a rather generic way, with parameters adapted to the case study. Also, the use of the co-simulation approach and FMI standard enables using the most adapted software to design each of them.

3.3.1. District-scale electric distribution network

This model is presented more in details in [14]. The electric network is scattered into subsystems such as:

- Building electric load using precalculated timeseries
- PV plants using solar irradiation and exterior temperature timeseries in order to provide their electricity production at each time step
- Electrical storage considering an electrochemical model and an inverter model
- Electrical grid consisting of a power balance of all components.

This model is implement using Matlab-Simulink [16] with a library of specific models dedicated to electric smart grid simulation.

3.3.2. District-scale heat production systems

Figure 2 from Rava et al. [14] describes the thermal model included into this work. This model is composed of four different type of energy systems:

- Controllable generators (P_i) such as cogeneration or heat pump
- Non-controllable generators (R_j) such as solar thermal field
- Storages (S_k) such as heat storage
- Load-tracking generator (LT) such as a gas boiler

In this model, the boundary conditions are the global heat set point imposed to generators by the controller (Q_{DHN}), and the inlet temperature (Tr_{DHN}) on the inlet side and the outlet temperature (Td_{DHN}). We consider a constant flow rate ($\dot{m}_{DHN}$)

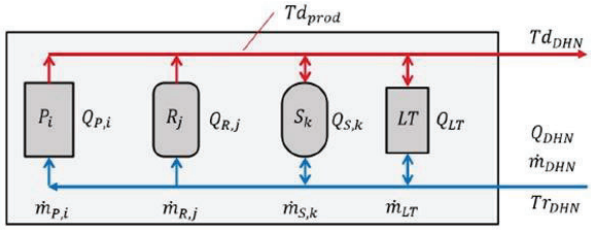

Figure 2. Schematic representation of the model of the thermal network production plant. (Source [14])

This model is implemented using Modelica [17], an object-oriented simulation tool that can simulate a various kind of thermo-dynamics simulation.

3.3.3. Buildings

Dynamic models are developed to represent several buildings of the district. Each building is considered as one thermal node. Given the footprint, the number of levels, the number of apartments and a global window area ratio of a building:

- The thermal zone is extruded from the footprint up to the total height of the building (3m by level)
- External surfaces are composed of layers with respect of typical thermal resistance values for French
- Building (typology LC24 in the PROFEEL project methodology)
    - Vertical surface : 5.3m².K/W;
    - Floor : 4.6m².K/W;
    - Ceiling : 6.5m².K/W;
- A global double glazing window is considered on each external surface with respect to the window ratio of the external surface;
- The 2012 French Thermal Regulation internal gains scenario, calculated according to the number of person in the building, is considered to reproduce the presence of inhabitants and their occupations;
- The air of the building is renewed considering air infiltration (1.2m3/h/m² @4Pa) and mechanical ventilation (0.3Vol/h).

Building simulations are carried out with the EnergyPlus software. EnergyPlus [17] is a validated and physicsbased Building Energy Simulation (BES) program used worldwide by researches, engineers and architects, and is developed by US Department of Energy. EnergyPlus building models are exported as FMUs using the energyplus-fmus export tool, considering the heat supplied by heat emitters as input, and the air, operative and ambient temperature as outputs.

3.3.4. Heat Distribution Circuit (HDC)

Since previous work [20] illustrated the impact of the thermal inertia of heat distribution circuits on flexible building control strategies, we included a detailed heat distribution circuit for each building in our simulation. Figure 3 represents the model of the secondary heat loop for each building.

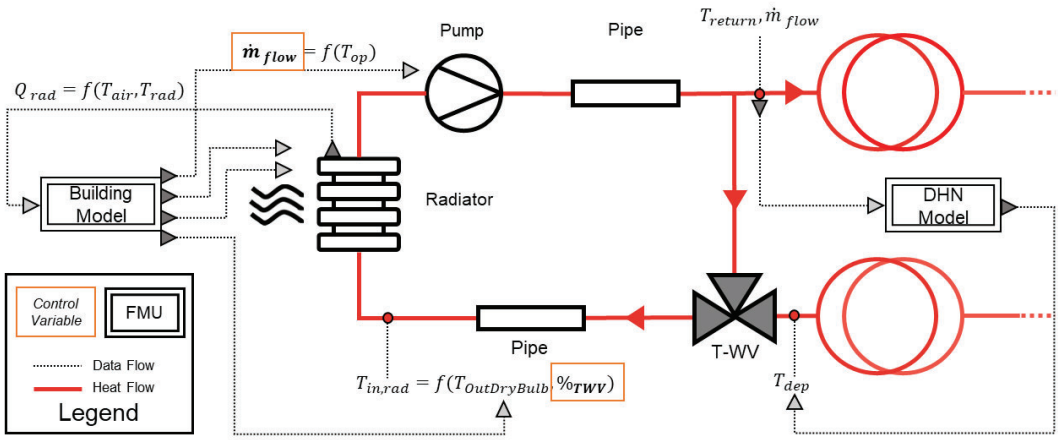

Figure 3. Schematic representation of the Heat Distribution Circuit model and its interaction with other models. (Source: Authors)

The model simulates the inertia of the distribution circuit and controls the building model temperature. It is composed of:

- A radiator providing heat to the thermal zone of the corresponding building (Q_{rad})
- A pump providing the proper flow rate (m_{flow}) to ensure the set point temperature
- A three-way valve (T_WV) used in order to control the input temperature of the radiator ($T_{in,rad}$) according to a heating law based on the outdoor temperature ($T_{OutDryBuld}$).
- Two pipes (after the valve and before the return loop) which simulate the inertia of the distribution circuit.

https://doi.org/10.52202/069564-0251

In addition, it takes into account the meta-control coming from the MILP model. Thus, a maximal value of heat is set to limit the heat provided to the building model according to the control strategy determine by the MILP model on the horizon.

3.4. Optimisation models for Model-Predictive Control

A Mixed Integer Linear Programming (MILP) model is used to compute an optimised strategy of control considering the overall multi-vector system. The MILP model is built using the in-house Persee software [20], which provides building blocks for multi-energy systems similarly to other tools, e.g. OmegAlpes [21].

3.4.1. MILP model for the Multi-energy networks

Figure 4 gives an overview of the MILP model of a multi-vector system based on previous work [15, 16].

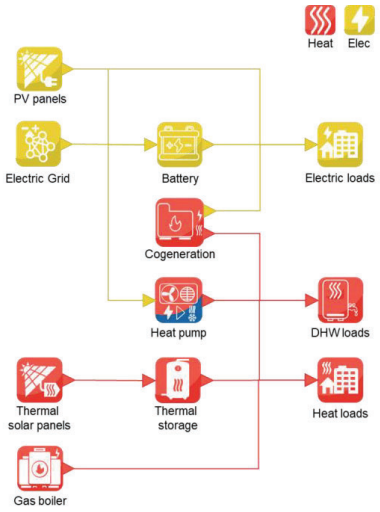

Figure 4. Design of an example of a complex multi-vector optimisation model at district scale. (Source: Authors)

The specificities of PERSEE enable the multi-vector modeling with complex system, including renewable energies. Using the model depicted by Figure 4 as an example, there are two energy vector:

- **Heat vector**
  - Production side
    - Thermal solar panels models: imposed thermal power injection into the system between min and max forecast time series
    - Gas boiler model: Thermal production from fuel gas into thermal
  - Storage side
    - Thermal storage: Storage model as a water tank considering energy power ○ Consumption side
    - Heat needs: imposed heat extraction from a pre-existing heat profile
    - DHW needs: imposed DHW extraction from a pre-existing DHW profile
- **Electric vector**
  - Production side
    - PV panels: imposed electrical power injection into the system, between min and max forecast time series
    - National electrical grid: computed flow injection or extraction to real or fictive grid
  - Storage side
    - Electro-chemical storage: batteries tank model with power map limitation
  - Consumption side
    - Electrical needs: imposed electric extraction from a pre-existing electric need profile
- **Coupling elements**
  - Heat pump: heat pump model consuming electricity to produce Heat and possible Cold
  - Cogeneration: thermal production from 3 input flows with optional electrical cogeneration

3.4.2. Flexible MILP model for flexible buildings

Figure 5 represents the building flexible MILP model implemented in PERSEE from previous work by Aoun et al. [22].

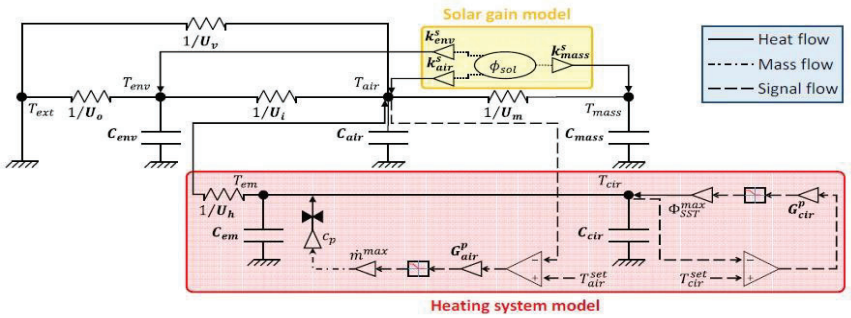

Figure 5. RC Model from which the building flexible MILP Model is inspired. (Source [24]) This model consists in the set of constraints and objective as follow (1):

$$min(dt^h.\sum_{t\in T}[c_T.\Phi_t + \Phi^{max}.c^{mean}.\Delta T_t + \lambda^{losses}.\Phi^{max}.c^{mean}.(T_t^{cir} - T_t^{air})])$$

$$\begin{cases} C^{air}.\frac{dT^{air}}{dt^s} = U_{air}^{ext}.(T_t^{ext} - T_t^{air}) + U_{air}^{env}.(T_t^{env} - T_t^{air}) + U_{air}^{mas}.(T_t^{mas} - T_t^{air}) + U_{air}^{em}.(T_t^{em} - T_t^{air}) + K_{air}.I_t^{sol} \\ C^{env}.\frac{dT^{env}}{dt^s} = U_{env}^{ext}.(T_t^{ext}(t) - T_t^{env}) + U_{air}^{env}.(T_t^{air} - T_t^{env}) + K_{env}.I_t^{sol} \\ C^{mas}.\frac{dT^{mas}}{dt^s} = U_{air}^{mass}.\left(T_t^{air} - T_t^{mas}(t)\right) + K_{mass}.I_t^{sol} \\ C^{em}.\frac{dT^{em}}{dt^s} = U_{air}^{em}.\left(T_t^{air} - T_t^{em}(t)\right) + \Psi_t \\ C^{cir}.\frac{dT^{cir}}{dt^s} = \eta^{cir}.\Phi_t - \Psi_t \\ \Psi_t \le m^{max}.cp.(T_t^{em}(t) - T_t^{cir}) \end{cases} \quad (1)$$

In this model, two distinct parts are considered:

- The building part where the air (T_{air} for the air temperature, C_{air} for the air capacity and K_{air} for the air solar gain factor), the building envelope (T_{env}, C_{env} and K_{env}), and the thermal mass of the building (T_{mas}, C_{mas} and K_{mas}) are modelled. The interactions between those thermal nodes and with the outdoor are taken into account with the thermal inductances (exterior/air (U_{air}^{ext}), envelope/air (U_{air}^{env}), mass/air (U_{air}^{mas})).
- The HDC part where the circuit (T_{cir} for the inlet circuit temperature, C_{cir} for the circuit capacity) and the emitter (T_{em} and C_{em}) are modelled, considering their interaction with the air via the emitter (U_{air}^{em}).

Φ_t represents the boundary condition with the heat transferred by the primary loop of the HDN and Ψ_t represents the heat transfer between the emitter and the circuit.

3.5. Calibration of the MILP model for Flexible buildings

Calibration of building model is a complex process. In this work, the MILP model needs to be calibrated to have similar thermal inertia as its EnergyPlus twin.

Figure 6 depicts the process of calibration applied on this study.

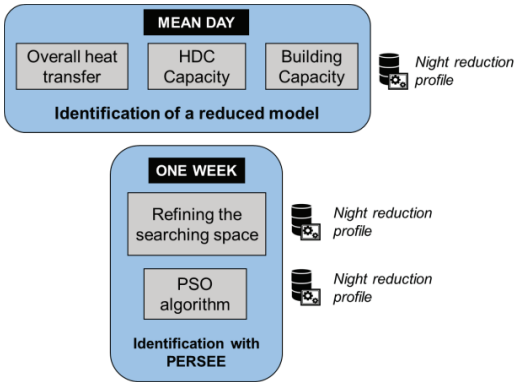

https://doi.org/10.52202/069564-0251

Figure 6. Process for calibration of optimization building model for flexibility (Source: Authors)

This calibration consists in two phases with two options for the second phase.

3.5.1. Phase one: initial parameters estimation

Figure 7 depicts the reduced model used in the phase one of calibration

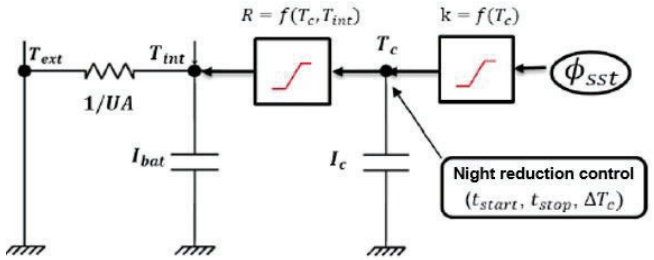

Figure 7. Reduced model used in the first phase of calibration process (Source: CEA)

This phase consists in the identification of the thermal parameter of the building considering this reduced model using a heat profile with night reduction as an input:

- The overall heat transfer coefficient of the building: determined in the night period following an empiric relation between this heat transfer coefficient and the difference between the indoor temperature and the outdoor temperature.

$$QHeat = UA.(Tindoor - Toutdoor) \quad (2)$$

- The total building capacity: determined using an empiric relation between the morning peak ($Q_{morning}$ when the setpoint passes from the night to the day mode) and the descending phase of the evening peak ($Q_{down,ve}$ when the setpoint temperature passes from the day to the night mode) and night and day setpoint temperatures (respectively T_{night} and T_{day}).

$$C_{building} = \frac{Q_{morning} - Q_{down,eve}}{T_{day} - T_{night}} \quad (3)$$

- The heat distribution circuit (HDC) capacity: determined by using an empiric linear relation with the descending phase of the evening peak.

$$C_{HDC} = \frac{Q_{down,eve}}{15} \quad (4)$$

- The solar coefficient aperture: determined by evaluating the total energy gain of the building during the solar period. Then, solar gain are obtained by subtracting the total energy the emitter heat and the internal gain from energy plus simulation.

$$K_{Building} = \frac{\mathrm{UA.(Tindoor - Toutdoor) - Q_{int} - Q_{heat}}}{\mathrm{Irr}} \quad (5)$$

The parameter of the reduced model are then used in order to give a first-phase value (FPV) for each parameter of the PERSEE building model. The table 2 details their relation:

Table 2. List of the energy system considered in this work.

Persee parameter	Relation with reduced model parameters
C^{air}, C^{env}, C^{mas}	$\frac{C_{building}}{3}$
C^{cir}, C^{em}	$\frac{C_{HDC}}{2}$
U_{air}^{ext}, U_{air}^{env}, U_{env}^{ext}, U_{air}^{mas}	$\eta_{Uxxx} * \mathrm{UA}$
K^{air}, K^{env}, K^{mas}	$\eta_K^{xxx} * \mathrm{K_{building}}$
U_{air}^{em}	$(\frac{\Phi_{heat}^{nom}}{\Delta T_{nom}})^{1.33}$ and $\Delta T_{nom} = \frac{T_{out,nom}^{em} + T_{out,nom}^{em}}{2} - T_{setpoint}^{air}$

η_{Uxxx} and η_K^{xxx} are extrapolating from the Building 2022 parameter in Table 2 of [24].

3.5.2. Phase two: refined parameter estimation

In order to refine the estimation of parameters, we use a Particle-Swarm Optimisation (PSO [23]) algorithm to identify the parameters using the MILP model for calibration. For a calibration assessment purpose, we choose a specific indicator, based on the root-mean-square error (RMSE) between observed and measured air temperature profiles and observed and measured heat profiles:

$$RMSE = \frac{rmse_{heat} + rmse_{temp}}{2}$$

$$rmse_{heat} = \frac{t_f}{\Delta t}\sqrt{\sum_{0}^{t_f} \frac{(\hat{\Phi}_{heat} - \Phi_{heat})^2}{max(\hat{\Phi}_{heat} - \Phi_{heat})}}$$

$$rmse_{temp} = \frac{t_f}{\Delta t}\sqrt{\sum_{0}^{t_f} \frac{(\hat{T}_{air} - T_{air})^2}{max(\hat{T}_{air} - T_{air})}}$$

The calibration with the MILP model in the loop consist in two steps. Figure 8 details the first step.

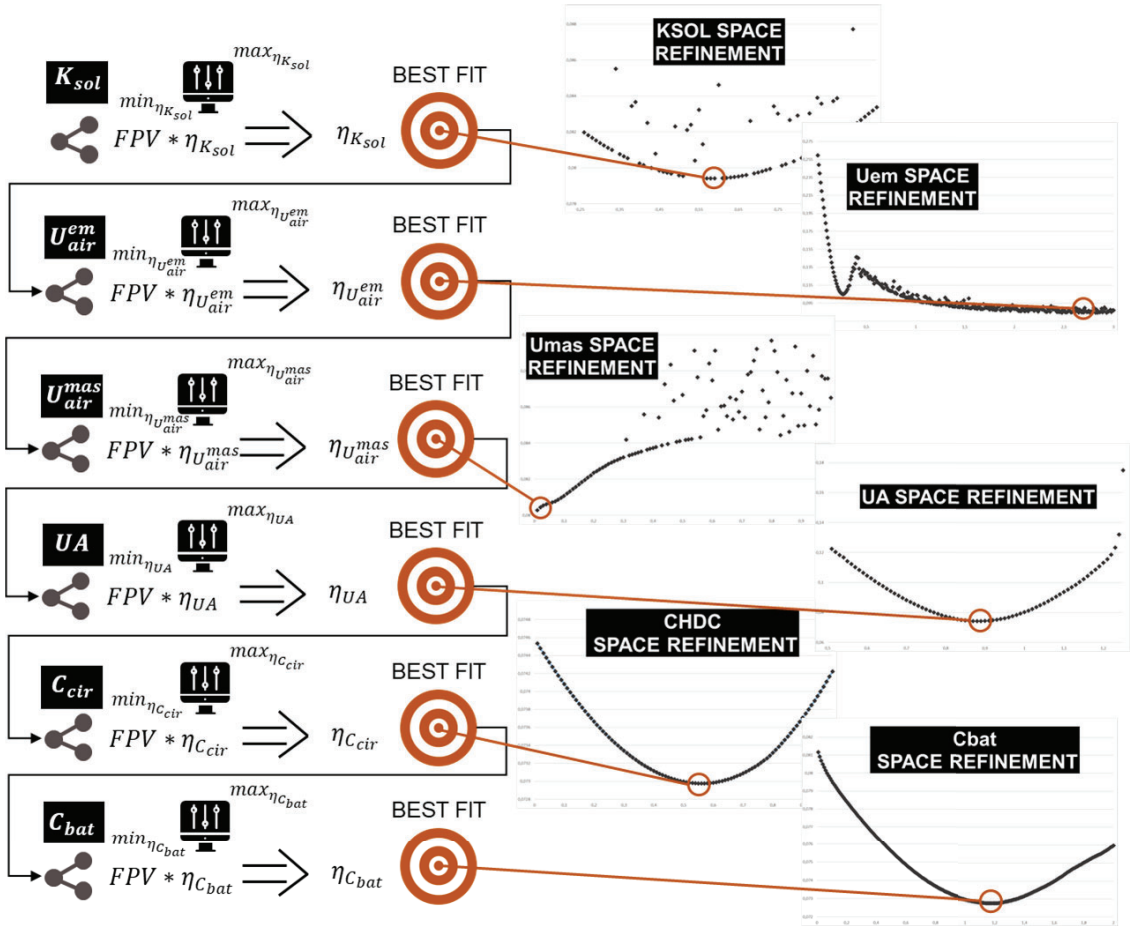

Figure 8. Heuristic method for refining the search step (Source: Authors)

At this stage, we aim to refine the search space for each parameter of the Persee model. The parameters are aggregated by their specificities as follow:

- Solar aperture coefficients (K^{air}, K^{env}, K^{mas}) are aggregated within K_{sol}
- U_{air}^{em} and U_{air}^{mas} are treated individually because of the specificity of their extrapolation.
- U_{air}^{ext}, U_{air}^{env}, U_{env}^{ext} are aggregated within UA
- C^{cir}, C^{em} are aggregated within C_{HDC}
- C^{air}, C^{env}, C^{mas} are aggregated within C_{bat}

https://doi.org/10.52202/069564-0251

Beforehand, the order of this heuristic algorithm has no importance, except for the solar aperture coefficient. Thus the error defers from the one from (6) by considering the RMS only during solar period. At each stage, the best-fit coefficient is selected from the assessment sample. This assessment sample is defined around the FPV. A discretization of the sample enables to assess 100 to 300 assessment in which we keep the value with the lowest RMSE. In the end, a new set of refined parameter is determined using their corresponding best-fit coefficient and their FPV.

4. Results

4.1. Simulation Hypothesis

- **Optimisation**: Considering the optimisation part, we consider a constraint in CO2 emission rate at district level of 20000kg and an economic objective function. The feed-in-tariffs of electricity consists in a conditioned one to day-and-night time slots.
- **MPC and cosimulation**: The horizon of the MPC, the time slots within the optimisation runs, is a 36 hours period. Both optimisation and simulation considers a 1 hour time step. Then, the co-simulation runs with a timeshift of 1 hours meaning that the control strategy is recalculated every timestep. The cosimulation runs during 60 days.
- **Thermal production**: On the thermal model part, the impact of the flexible building on its flowrate is neglected. We consider it as a constant value. The overall district heat production is adapted by considering the building flexible integrated in the district. The heat profile of each flexible building is subtracted from the district heat profile.
- **Building model**: At our current state of work, we consider a monozone building model and HDC model. Considering multi-zone building model in order to evaluate its effect on the calibration and flexibility is a perspective for further studies. 8 building on the 13 are modelled.
- **Calibration**: The full calibration process is set for five buildings; the first heuristic results are applied on others.

4.2. Calibration Results

For this case study, we applied the full calibration process presented in section 3.5. for the five main buildings. For the three last, the process end at the heuristic step of the second phase. In order to evaluate the calibration performances, the table 3 records the RMS for each building at each stage, in addition with a test of the performance of PSO algorithm using the unrefined search space. Considering the two PSO, we defined their search space giving the same minimal and maximal coefficient.

Table 3. Recording of RMS during the calibration process.

Buildings	RMSE with FPV	RMSE after refinement	RMSE with unrefined PSO	RMSE with refined PSO
CastelO	0.09359	0.06114	0.08039	0.06089
Panache	0.10103	0.07276	0.08729	0.07303
Python	0.07741	0.03935	0.06536	0.03924
Up	0.11137	0.09039	0.09707	0.0857
Zenae	0.09712	0.03566	0.07720	0.03453
Novae	0.05511	0.03210	-	-
Thales	0.07851	0.03514	-	-
Soleil	0.06842	0.06130	-	-

Figure 9 focuses on the two extreme buildings

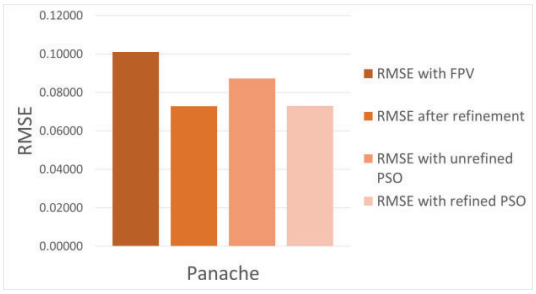

(a)

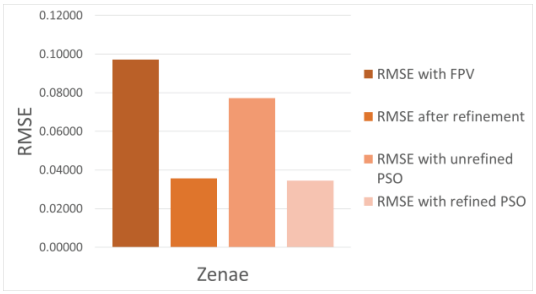

(b)

Figure 9. Focus on two buildings a) building obtaining the worst amelioration with refining b) building obtaining the best amelioration with refining (Source: Authors)

At this stage, the refining seems to have a positive effect on the global error, considering the chosen indicator. At best case, the amelioration is around 60% from the first phase calibration with a mean value of 38% with the heuristic algorithm and 40% with refined PSO. The worst case is interesting because the PSO algorithm have found a slightly less performant set of parameter than the heuristic algorithm. Moreover, the gain from PSO is a mean of two point compared to the heuristic. Two possibilities can explain this fact. Firstly, the heuristic algorithm differs from the PSO on the solar aperture assessment. Indeed, for the heuristic algorithm, we have chosen to evaluate only the solar timeslots as those coefficients have no effect without solar irradiation on the model. Secondly, we have neglected a proper study on the configuration of the PSO, which could lead to underestimated performances. Section 4. Presents areas of improvement considering the calibration phase.

4.3. Co-simulation results

The main difficulty for the MILP model is to determine the flexibility coefficient for each flexible building model. This coefficient is set first using a standalone optimisation on the horizon time. Figure 10 shows the result for the chosen flexibility coefficient.

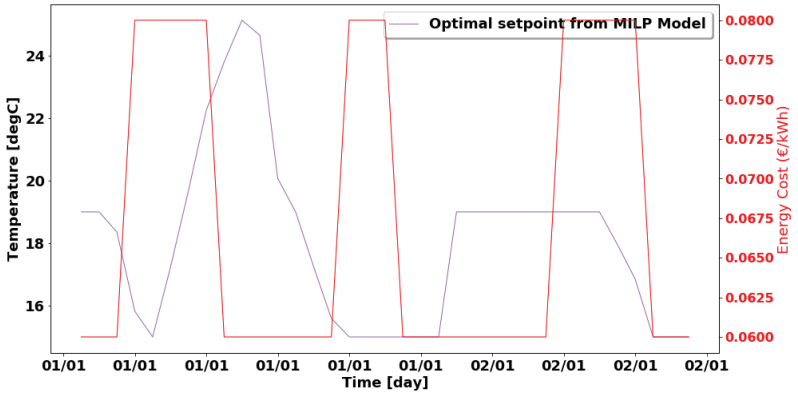

Figure 10. Optimal Air temperature from MILP Model on the horizon time (Source: Authors)

The multi-vector system is quite complex, leading to a difficulty to find a satisfying value for this coefficient. We applied this flexibility coefficient for the co-simulation. To give an idea of time solving for one building, a co-simulation with one building takes 8 minutes to run and 23 minutes with 8 buildings

Figure 11 shows the results concerning the co-simulation for one building.

https://doi.org/10.52202/069564-0251

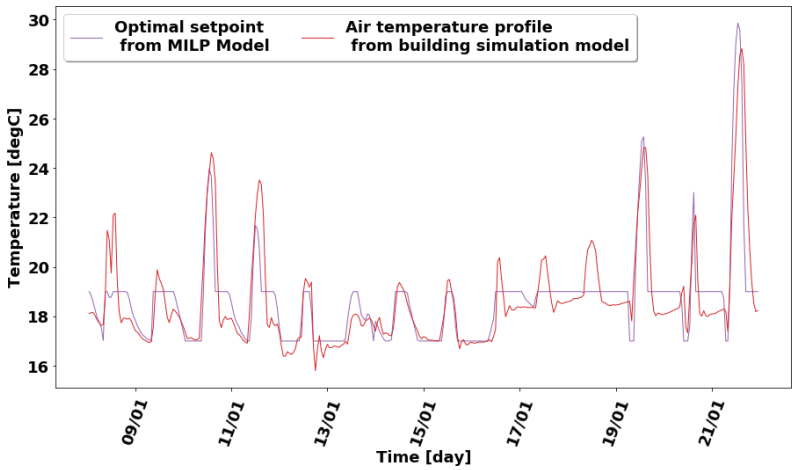

Figure 11. Set point temperature from MILP model profile and air temperature profile from building model (Source: Authors)

At this stage, we can obtain an effect on the temperature set point of EnergyPlus building model. However, those results aren't satisfying enough for one building and are the same kind for eight buildings. Further improvements would be necessary to obtain solid results at district scale.

5. Conclusion

This article presents a co-simulation procedure in order to process a flexibility assessment building by building. This co-simulation embeds an electric simulation model, a thermal model composed of a thermal production model, a heat distribution circuit model and a building model and a MILP model optimizer ensures MPC. The first aim is to calibrate the building models in order to implement them for co-simulation. A proper calibration procedure has been implemented with a satisfactory accuracy. Then we could test the co-simulation from one to eight buildings at district scale.

For future work, the calibration process could be improved by assess the configuration of the PSO algorithm on the one hand. On the other hand, the PSO process could be improved by splitting the search of solar aperture coefficients from the other parameters. In doing so, we could hope obtaining better results for calibration. Then, a better training phase could be implemented to refine the calibration process. On the co-simulation side, we would have to improve the flexibility coefficient study in order to find a procedure to set it. Another option that we would like to study is to reduce the time step from one hour to 10 minutes. Indeed, as we obtain decent computing time, this seems to be feasible. Reducing the time step of co-simulation could improve the sensitivity of the flexible building model and help to find a better flexibility coefficient.

6. References

[1] Sarbu I, Mirza M, Muntean D. 2022. Integration of Renewable Energy Sources into Low-Temperature District Heating Systems: A Review. Energies 15:6523.

[2] Onen PS, Mokryani G, Zubo RHA. 2022. Planning of Multi-Vector Energy Systems with High Penetration of Renewable Energy Source: A Comprehensive Review. Energies 15:5717.

[3] Chaudhary G, Lamb JJ, Burheim OS, Austbø B. 2021. Review of Energy Storage and Energy Management System Control Strategies in Microgrids. Energies 14:4929.

[4] M. González-Torres, L. Pérez-Lombard, Juan F. Coronel, Ismael R. Maestre, Da Yan, A review on buildings energy information: Trends, end-uses, fuels and drivers, Energy Reports, Volume 8, 2022, Pages 626-637

[5] Lavinia Marina Paola Ghilardi, Alessandro Francesco Castelli, Luca Moretti, Mirko Morini, Emanuele Martelli, Co-optimization of multi-energy system operation, district heating/cooling network and thermal comfort management for buildings, Applied Energy, Volume 302, 2021, 117480, ISSN 0306-2619

[6] J. Kozadajevs and D. Boreiko, "District Heating System Flexibility Studies Using Thermal Inertia of Buildings," 2020 IEEE 61th International Scientific Conference on Power and Electrical Engineering of Riga Technical University (RTUCON), Riga, Latvia, 2020, pp. 1-5

[7] Yang Li, Chunling Wang, Guoqing Li, Jinlong Wang, Dongbo Zhao, Chen Chen, Improving operational flexibility of integrated energy system with uncertain renewable generations considering thermal inertia of buildings, Energy Conversion and Management, Volume 207, 2020

[8] Q. Gao, M. Demoulin, H. Wang, S. Riaz and P. Mancarella, "Flexibility Characterisation from Thermal Inertia of Buildings at City Level: A Bottom-up Approach," 2020 55th International Universities Power

Engineering Conference (UPEC), Turin, Italy, 2020, pp. 1-6
[9] Vandermeulen, Annelies & Reynders, Glenn & van der Heijde, Bram & Vanhoudt, D. & Salenbien, Robbe & Saelens, Dirk & Helsen, L.. (2018). Sources of Energy Flexibility in District Heating Networks: Building Thermal Inertia Versus Thermal Energy Storage in the Network Pipes.
[10] Zhaoguang Pan, Qinglai Guo, Hongbin Sun, Feasible region method based integrated heat and electricity dispatch considering building thermal inertia, Applied Energy, Volume 192, 2017, Pages 395-407
[11] Optimal scheduling strategy of district integrated heat and power system with wind power and multiple energy stations considering thermal inertia of buildings under different heating regulation modes Dan Wang et al. Applied Energy 240 (2019) 341-358.
[12] Collaborative scheduling and flexibility assessment of integrated electricity and district heating systems utilizing thermal inertia of district heating network and aggregated buildings Xue Li et al. Applied Energy, 258 (2020)
[13] Pajot C, Artiges N, Delinchant B, Rouchier S, Wurtz F, Maréchal Y. 2019. An Approach to Study District Thermal Flexibility Using Generative Modeling from Existing Data. Energies 12:3632.
[14] Rava L., Wantier W., Vallée M., Alain R., Nicolas L., Assessment of Varying Coupling Levels between Electric & Thermal networks at District Level using Co-Simulation and Model-predictive Control. Smart Energy, Volume 6, 2022, 919-930.
[15] Fitó J., Vallée M., Ruby A., Cuisinier E., Robustness of district heating versus electricity-driven energy system at district level: A multi-objective optimization study, Smart Energy, Volume 6, 2022, 100073.
[16] Blochwitz, T., Otter, M., Åkesson, J. Arnold, M., Clauss, C., Elmqvist, H., Friedrich, M., Junghanns, A., Mauss, J., Neumerkel, D., Olsson, H., Viel, A. (2012). Functional Mockup Interface 2.0: The Standard for Tool independent Exchange of Simulation Models. Proceedings.
[17] Zhicheng X., Chuang Z., Bo Sun, SuZhen L., The electric-thermal coupling simulation and state estimation of lithium-ion battery, ournal of Energy Storage, Volume 58, 2023, 106431.
[18] Elmqvist, H., & Mattsson, S. E. (1998). An Overview of the Modeling Language Modelica. Paper presented at Eurosim'98 Simulation Congress, Helsinki, Finland.
[19] Crawley, D., Pedersen, C., Lawrie, L., Winkelmann, F. (2000). EnergyPlus: Energy Simulation Program. Ashrae Journal. 42. 49-56.
[20] Nadine Aoun, Roland Bavière, Mathieu Vallée, Antoine Aurousseau, Guillaume Sandou, Modelling and flexible predictive control of buildings space-heating demand in district heating systems, Energy, Volume 188, 2019, 116042.
[21] Cuisinier, E., Lemaire, P., Penz, B., Ruby, A., Bourasseau, C., (2021). New rolling horizon optimization approaches to balance short-term and long-term decisions: An application to energy planning. Energy.
[22] Hodencq S, Brugeron M, Fitó J, Morriet L, Delinchant B, Wurtz F. 2021. OMEGAlpes, an Open-Source Optimisation Model Generation Tool to Support Energy Stakeholders at District Scale. Energies 14:5928.
[23] Aoun, N., Bavière, R., Vallée, M., Sandou, Ge. (2019). Development and assessment of a reduced-order building model designed for model predictive control of space-heating demand in district heating systems.
[24] Gad, A. (2022). Particle Swarm Optimization Algorithm and Its Applications: A Systematic Review. Archives of Computational Methods in Engineering. 29.

 https://doi.org/10.52202/069564-0251